Zn doping effect on the superconducting gap in $YBa_2Cu_3O_{7-\delta}$: Raman study

M. Limonov,* D. Shantsev,* and S. Tajima
SRL-ISTEC, 10-13, Shinonome 1-Chome, Koto-ku, Tokyo 135-0062, Japan

A. Yamanaka
Chitose Institute of Science and Technology, Chitose, Hokkaido 066-8655, Japan

(Received 26 February 2001; revised manuscript received 7 August 2001; published 19 December 2001)

The Raman scattering spectra of twin-free $YBa_2(Cu_{1-x}Zn_x)_3O_{7-\delta}$ single crystals with an optimal oxygen content ($T_c = 93$ K at $x = 0$) have been investigated in a temperature range from 300 to 10 K in *YY* and *X′Y′* polarizations. Below T_c, we found a low-frequency shift of the gap-related peak in the electronic response with Zn doping, accompanied by broadening. The changes in the phonon renormalization effects are consistent with the change in the electronic response. All the observed Zn-doping effects can be roughly described in the theoretical model for a *d*-wave superconductor in a unitarity limit.

DOI: 10.1103/PhysRevB.65.024515 PACS number(s): 74.25.Gz, 74.25.Kc, 74.72.Bk

I. INTRODUCTION

Pair breaking due to impurity doping is an important issue to discuss when considering the mechanism of high-T_c superconductivity. The effects of a nonmagnetic impurity on superconductivity were theoretically predicted for a *d*-wave superconductor.[1,2] The predictions were examined by many experimental investigations such as NMR[3,4] resistivity,[5] surface impedance,[6] electronic specific heat,[7] optical spectra,[8,9] neutron scattering,[10] muon spin rotation,[11] and Raman-scattering studies.[12–15] Although a T_c depression with impurity doping can be understood in terms of the pair breaking due to strong potential scattering in a *d*-wave superconductor, the reduction in a superfluid density[6,9,11] deviates quantitatively from conventional theory. This is partly explained by assuming a local destruction of superconductivity around impurities. In fact, recent results of a scanning tunneling microscope (STM) measurement[16] revealed intense quasiparticle resonance peaks within 15 Å around Zn sites, demonstrating that superconductivity is locally destroyed. Such an inhomogeneous pair-breaking state is not compatible with a conventional homogeneous picture. Therefore, we need to interpret much of the experimental data in the context of average information.

In contrast to the determination of T_c and the superfluid density, it is more difficult to determine the superconducting gap energy in high-T_c superconductors (HTSC's). Experimental techniques by which the gap value can be determined are limited to, for example, tunneling spectroscopy and photoemission spectroscopy. However, there has been no clear tunneling and photoemission data which includes the impurity-doping effect on the gap magnitude. Another probe for a gap measurement is a Raman-scattering spectroscopy.

In a normal state, the Raman spectra of optimally doped HTSC's show a flat background due to the electronic scattering. Below T_c this broad electronic continuum redistributes into the so-called 2Δ peak associated with the breaking of Cooper pairs.[17] One of the major difficulties in the study of the 2Δ peak is that this peak is usually superimposed by several phonon lines, which are also temperature dependent. Moreover, the strong electron-phonon coupling leads to a strong renormalization of the phonon line parameters below T_c,[18,19] making the separation of electronic and phononic components in Raman spectra even more difficult. In particular, for $YBa_2Cu_3O_{7-\delta}$ (YBCO) crystals there are several phonon lines near the 2Δ peak, and the strongest B_{1g}-like phonon line at 340-cm^{-1} shows very pronounced renormalization effects in all parameters—frequency, linewidth, and intensity.[20] Therefore, a proper separation of electronic and phononic components in Raman-scattering spectra is of great importance.

Concerning Raman studies of Zn effects on the superconducting gap, there was a preliminary work by Matic *et al.*,[13] although they found a clear Zn-doping effect only on the A_{1g} spectra but not on the B_{1g} spectra. Altendorf *et al.* observed a surprisingly huge effect of Th doping on both the A_{1g} and B_{1g} spectra of $YBa_2Cu_3O_7$ in spite of only a 0.5-K reduction in T_c by Th doping.[12] Therefore, a further investigation is desirable, using well-characterized samples. In this study, we performed precise Raman measurements of the optimally doped twin-free $YBa_2(Cu_{1-x}Zn_x)_3O_{7-\delta}$ single crystals in both A_{1g} and B_{1g} polarizations. The Raman spectra were investigated for various temperatures, polarizations, excitation energies, and doping levels. To extract uncoupled electronic and phonon parameters and interference effects, we improved our Green's-function approach,[21] assuming an appropriate electronic response function where real and imaginary parts are connected via the Kramers-Kronig relation. Applying this model for analysis of the Raman spectra, we demonstrate the Zn-substitution effects on the behavior of the 2Δ peak in B_{1g} polarization as well as on the phonon self-energy. A reduction in the gap amplitude $2\Delta(T)$ by Zn doping was clearly seen both in the electronic and phononic Raman scattering with B_{1g} symmetry.

II. EXPERIMENT

High-quality $YBa_2(Cu_{1-x}Zn_x)_3O_{7-\delta}$ single crystals with $x = 0$ and 0.004 were grown by a top-seeded pulling technique, and oxygenated under uniaxial pressure in order to obtain the orthorhombic twin-free samples, as was described previously.[22] The Zn-free crystals have the optimal T_c of 93

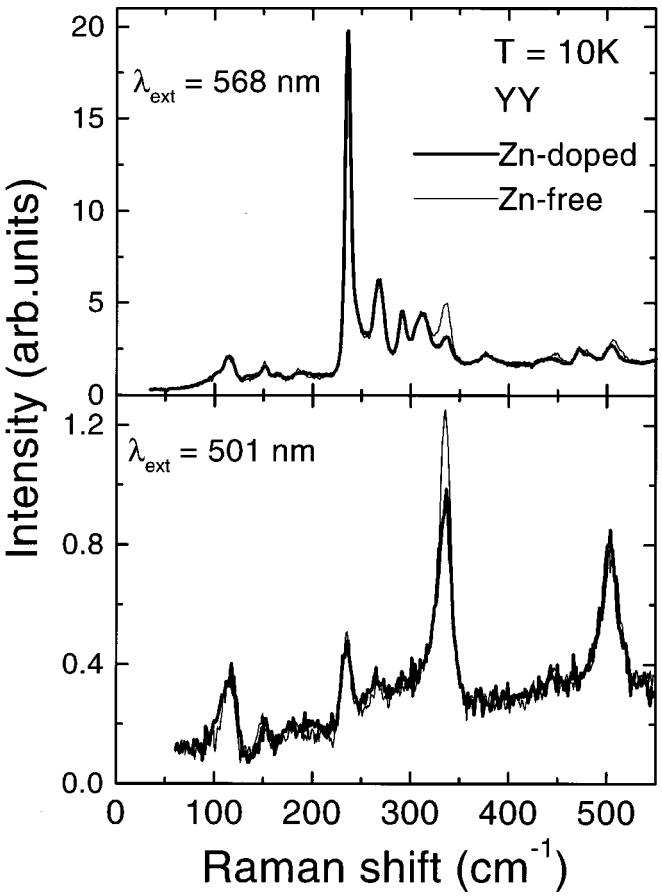

FIG. 1. The *YY*-polarized Raman spectra of detwinned Zn-free and Zn-doped $YBa_2(Cu_{1-x}Zn_x)_3O_{7-\delta}$ crystals at $T=10$ K taken with $\lambda_{ext}=568$ nm and 501 nm.

K with a very narrow transition width $\Delta T_c \leqslant 0.2$ K. The Zn-doped YBCO was annealed in the same conditions as the Zn-free one, and therefore expected to have the optimal oxygen content. The T_c value is reduced down to 85 K by Zn doping. The Zn concentration was determined by inductively coupled plasma spectrometry.

The Raman spectra were studied using a T64000 Jobin-Ivon triple spectrometer with a liquid-nitrogen cooled CCD detector. The typical spectral resolution was 3 cm^{-1}. The Raman spectra were obtained in pseudobackscattering geometry in *XX* and *YY* polarizations ($A_{1g}+B_{1g}$ components are dominant in orthorhombic YBCO crystals), as well as in the $X'Y'$ polarization (B_{1g} is dominant). We used several Ar^+-Kr^+ laser lines ranging from red excitation with an energy of 1.92 eV ($\lambda_{exc}=647.1$ nm) to blue excitation with an energy of 2.60 eV ($\lambda_{exc}=476.5$ nm). The power density was about 1 W/cm^2 on the sample surface, and, as a result, the sample heating was less than 10 K in all experiments.

III. RESULTS

Figure 1 presents the *YY*-polarized Raman spectra of the Zn-free and Zn-doped YBCO crystals at $T=10$ K. The A_g Raman modes for the $YBa_2Cu_3O_7$ lattice are dominant in the spectra for $\lambda_{ext}=501$ nm. Hereafter, we refer to the five well-known A_g lines as the 120-, 150-, 340-, 430-, and 500-cm^{-1} lines. The low-frequency lines at 120 and 150 cm^{-1} are ascribed mainly to *Z* displacements of Ba and planar Cu(2), respectively. The 340-cm^{-1} mode belongs to B_{1g} symmetry in the tetragonal $YBa_2Cu_3O_6$ structure (point group D_{4h}) with out-of-phase O(2) and O(3) oxygen displacements along the *Z* direction. The 430-cm^{-1} line is mainly due to the in-phase *Z* displacements of the O(2) and O(3) oxygen atoms, and the 500-cm^{-1} one is associated with the apical oxygen O(1) displacements along the *Z* axis.

In the *YY* polarization there are several additional lines associated with the oxygen-deficient Cu(1)O(4) chains along the *Y* axis. The most intense line at about 230 cm^{-1} is assigned to vibrations of Cu(1) atoms. It is well known that the resonance effect is dramatic in the *YY* polarization,[23,24] in particular for $\lambda_{ext}=568$ nm the ''defect'' lines are noticeably enhanced. For example, the 230-cm^{-1} line exhibits a sharp resonance effect, suggesting the existence of a narrow electron band with an energy of about 2.2 eV.

Comparing the two spectra of Zn-free and Zn-doped samples, we found that only the 340-cm^{-1} line decreases its intensity by Zn doping, but all other lines show no Zn-doping effect on the intensity and the resonance behavior. Since the resonance behavior of the ''defect'' lines is very sensitive to the oxygen content,[24] the results of Fig. 1 provide evidence that the annealing procedure was identical, giving almost the same oxygen content in the Zn-free and Zn-doped YBCO.

The Raman spectra in the $X'Y'$ polarization consist of an electronic continuum, the 340-cm^{-1} B_{1g}-like phonon line and several weak A_{1g}-like phonon lines. To simplify the analysis, we subtract the minor A_{1g}-like phonon lines. Figure 2 shows the $X'Y'$ spectra for Zn-free and Zn-doped crystals after this subtraction. In the normal state, there seems to be a slight difference between the spectra of the Zn-free and Zn-doped crystals. In contrast, below T_c the superconductivity-induced spectral changes are strongly modified by the Zn doping. In Zn-doped crystals, the 340-cm^{-1} line becomes small and broad, while the peak in the electronic background shifts toward lower frequencies and the Raman intensity below 300 cm^{-1} becomes larger.

IV. ANALYSIS

To discuss the Zn-doping effects in the Raman spectra quantitatively, we need to separate the electronic and phononic components which couple with each other. There are several approaches for extraction of the electronic background from the Raman spectrum.[20,25–30] The first one is the widely used ''standard Fano procedure.'' This approach allows us to extract renormalized phonon parameters without determining electronic parameters (see the Appendix). To extract electronic parameters together with bare phonon parameters, a more complicated approach is needed, e.g., one based on a Green's-function analysis. In the following analysis, we extract the electronic response function $\chi(\omega)=R(\omega)+i\rho(\omega)$, and phonon parameters such as frequency and linewidth. Based on the Green's-function operator approach, an

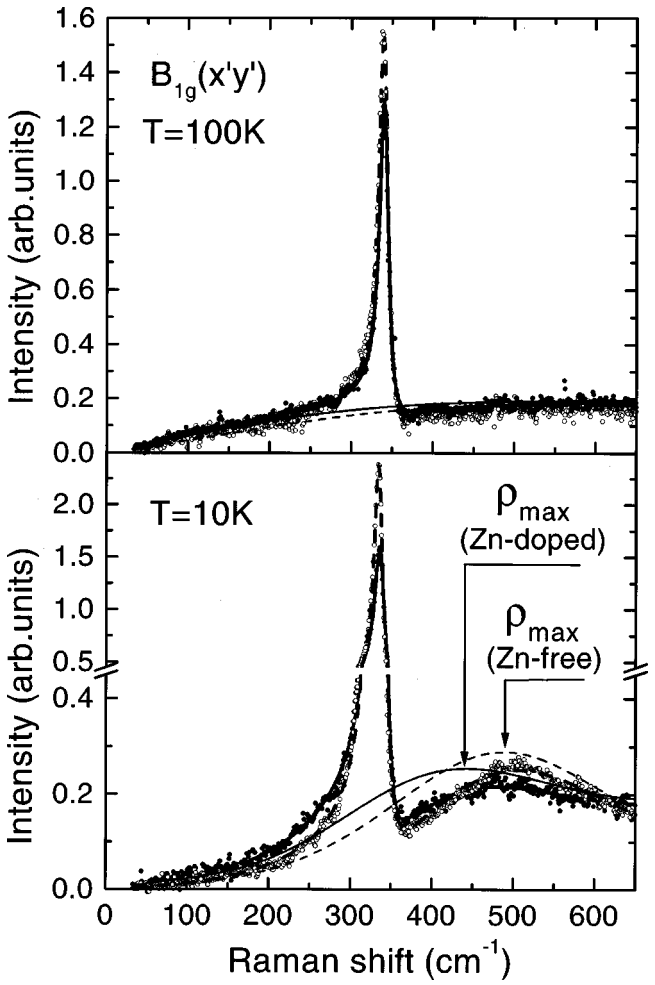

FIG. 2. The Raman spectra of the $YBa_2(Cu_{1-x}Zn_x)_3O_{7-\delta}$ crystals at temperatures above and below T_c in the B_{1g} polarization after subtraction of A_{1g}-like phonons. Open (solid) symbols show experimental data for Zn-free (Zn-doped) crystals; thick curves are the fitting results. The thin curves show $\rho(\omega)$.

expression is proposed for the coupled Raman spectrum:[25]

$$I(\omega)=[1+n(\omega)]\left\{\rho(\omega)+\frac{1}{\Gamma(1+\varepsilon^2)}\times\left[\frac{S^2}{V^2}+2\rho(\omega)\varepsilon S-\rho^2(\omega)V^2\right]\right\}, \quad (1)$$

where $1+n(\omega)=1+1/[\exp(\hbar\omega/k_BT)-1]$ is the Bose factor, $\varepsilon=(\omega-\Omega)/\Gamma$, and $S=S_0+V^2R(\omega)=VT_p/T_e+V^2R(\omega)$. Here V is the electron-phonon coupling, T_p is the Raman matrix element ascribed to transitions from the ground state to a one-phonon excited state, and T_e is the Raman matrix elements ascribed to the transitions to a continuous distribution of the excited electronic states. The renormalized frequency Ω and the linewidth Γ of the phonon are given by $\Omega=\Omega_0+V^2R(\omega)$ and $\Gamma=\Gamma_0+V^2\rho(\omega)$, where Ω_0 and Γ_0 are uncoupled values. The first term in Eq. (1), $\rho(\omega)$, represents the pure electronic continuum, the second term reflects the phonon contribution, and the last two terms result from the coupling effects. The resonance character of the light scattering is taken into account in calculation of the Raman matrix elements T_p and T_e.

For a complete analysis, it is necessary to assume a proper function of the electronic response $\chi(\omega)=R(\omega)+i\rho(\omega)$. In the normal state, the imaginary part $\rho_n(\omega)$ is determined by an incoherent electronic background. For $\rho_n(\omega)$, Bock *et al.*[29] proposed a phenomenological expression $\tanh(\omega/\omega_T)$. We examined several other formulas for $\rho_n(\omega)$, and found that the following simple expression successfully describes the spectra:

$$\rho_n(\omega)=C_n\frac{\omega}{\sqrt{\omega^2+\omega_T^2}}, \quad (2)$$

where C_n and ω_T are the fitting parameters. This function satisfies the requirement for the normal electronic response function, i.e., $\rho_n(\omega)=\text{const}$ at $\omega\rightarrow\infty$ and $\rho_n(\omega)\propto\omega$ at $\omega\rightarrow 0$.

At temperatures below T_c, it is convenient to write down the total electronic response as a sum of the normal and superconducting contributions, $\rho(\omega)=\rho_n(\omega)+\rho_s(\omega)$. The superconducting contribution $\rho_s(\omega)$ should reflect the appearance of a superconducting gap leading to a peak which is accompanied by a suppression of $\rho(\omega)$ at lower frequencies. Both the peak and suppression are described by Lorentzians with opposite signs similar to those proposed in Ref. 29. The real part $R(\omega)$ is directly linked to the imaginary part $\rho(\omega)$ via the Kramers-Kronig relation (for details, see Ref. 15). Note that $R(\omega)$ also enters the basic Equation (1) through Ω and S; thus our procedure allows a fully self-consistent treatment of the spectra.

This procedure based on Eq. (1) was used to fit the present Raman spectra in the XX and $X'Y'$ polarizations (A_{1g}- and B_{1g}-like scattering channels). We used four ω-independent fitting parameters Ω_0, Γ_0, S_0, and V, as well as two functions $\rho(\omega)$ and $R(\omega)$ which are connected via Kramers-Kronig relation. Hereafter we will mainly focus on the Raman spectra in the B_{1g} polarization, since the d-wave gap amplitude is maximized in this symmetry, and thus the Zn-doping effect must be most sensitively detected. The fitting results for the A_{1g} spectra were reported in our previous paper.[14]

V. DISCUSSION

First we consider the Zn-doping effect on the electronic component in the Raman spectra. The $X'Y'$ spectra were analyzed on a basis of Eq. (1). The fitting curves at 100 and 10 K are shown in Fig. 2. In this fitting procedure, the electronic response $\chi(\omega)=R(\omega)+i\rho(\omega)$ are determined at each temperature. In the normal state, the slope of $\rho(\omega)$ at $\omega\rightarrow 0$ gives the inverse of the carrier scattering rate. From Eq. (2), it is expected that ω_T/C_n represents the scattering rate. It was found that the obtained parameter ω_T/C_n is about three times larger in the Zn-doped YBCO than in the Zn-free YBCO at all temperatures. This is consistent with the resis-

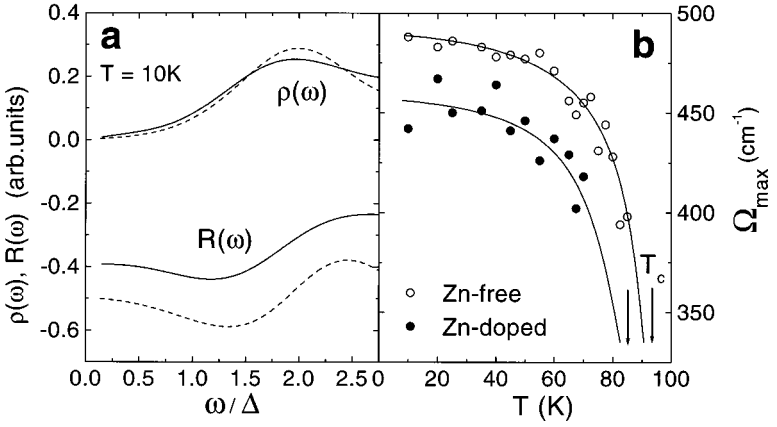

FIG. 3. (a) Real and imaginary parts of the electronic response $\chi(\omega)=R(\omega)+i\rho(\omega)$ at $T=10$ K. Dashed (solid) curves correspond to Zn-free (Zn-doped) crystals. (b) The temperature dependences of the frequency for the maximum of the electronic response function $\rho(\omega)$ in the B_{1g} polarization for the Zn-free and Zn-doped $YBa_2(Cu_{1-x}Zn_x)_3O_{7-\delta}$ crystals. The solid lines are guides for the eye.

tivity data, which shows a T-independent increase with Zn-doping due to potential scattering.

When the temperature is lowered below T_c, a broad peak appears in the Raman spectra as a result of the superconductivity induced redistribution of the electronic continuum $\rho(\omega)$.[17] This electronic peak is associated with a breaking of Cooper pairs, and, depending on the scattering polarization, is located at frequencies $\omega \leqslant 2\Delta_{\max}$, where $\Delta_{\max}$ is amplitude of the superconducting gap. In the case of B_{1g} polarization the peak is located at $2\Delta_{\max}$.[31]

In Fig. 3(a), the obtained spectra of $R(\omega)$ and $\rho(\omega)$ at 10 K are presented. At 10 K, the peak is centered at a frequency of about 490 cm^{-1} ($\sim 7.5kT_c$) for the Zn-free YBCO and at about 460 cm^{-1} ($\sim 7.7kT_c$) for the Zn-doped YBCO. This result suggests that the gap amplitude $2\Delta(T=0)$ roughly scales with T_c, as was pointed out by Matic *et al.*[13] The temperature dependence of the peak frequency $\Omega_{\max}$ is presented in Fig. 3(b). A difference in the gap amplitude $2\Delta(T)$ between Zn-free and Zn-doped crystals can be clearly seen at all temperatures, in as much as this electronic peak is resolved in the Raman spectra. Nearly the same Zn-substitution effect on the response function $\rho(\omega)$ was observed for the A_{1g} channel, as reported in our previous paper,[14] while the gap amplitude in the A_{1g} polarization is smaller than in the B_{1g} polarization.

Next we discuss the phonon parameters, which also reflect the electronic changes. In Fig. 4 we plot temperature dependencies of the coupled (Ω, Γ, and S) and uncoupled (Ω_0, Γ_0, and S_0) phonon parameters for the 340-cm^{-1} line. In the normal state, all phonon parameters of the 340-cm^{-1} line are nearly the same for the Zn-free Zn-doped YBCO crystals. However, below T_c phonon self-energy effects are different between these two samples because of the weaker renormalization effects in Zn-doped crystals.

The uncoupled frequencies Ω_0 show a smooth temperature dependence, following the curve described by a simple two-phonon-decay model:[32]

$$\Omega_0(T)=\Omega(T_0)-C_1[1+2n(\omega/2,T)], \tag{3}$$

where

$$n(\omega/2,T)=1/[\exp(\hbar\omega/2k_BT)-1].$$

This result indicates that electronic and phononic contributions to the spectra have been separated successfully.

The renormalized frequencies $\Omega=\Omega_0+V^2R$ show a small softening ($|V^2R|\sim 2$ cm^{-1}), due to interaction with the electronic background even in the normal state. The superconductivity induced effect manifests itself in a rapid decrease of the renormalized frequencies Ω below T_c. The magnitude of softening of the 340-cm^{-1} line is appreciably changed with Zn doping, reflecting a change in $R(\omega)$ as shown in Fig. 3(a). For the Zn-free crystal, a step like softening of the renormalized frequency Ω occurs between 90 and 50 K, and almost saturates below 50 K. The total softening is about 6 cm^{-1} [(Fig. 4(a)], which is in good agreement with the earlier Raman studies of YBCO crystals with an optimal oxygen content.[21,33] In a Zn-doped crystal, the softening becomes

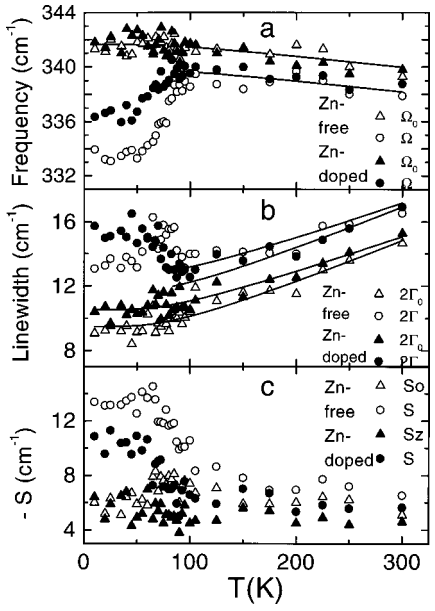

FIG. 4. Temperature dependences of the fitting parameters of the 340-cm^{-1} phonon for Zn-free and Zn-doped single crystals. (a) The uncoupled frequencies Ω_0 and renormalized frequencies $\Omega=\Omega_0+V^2R$. (b) The uncoupled linewidth $2\Gamma_0$ and renormalized linewidth $2\Gamma=2(\Gamma_0+V^2\rho)$. (c) The uncoupled parameter S_0 and renormalized parameter $S=S_0+V^2R$. The solid lines in (a) and (b) are the fitting curves calculated by a two-phonon-decay model [Eqs. (3) and (4)].

smaller, being about 4 cm^{-1}, which implies that $|R|$ at $\omega = 340\,cm^{-1}$ becomes smaller. This is consistent with the result in Fig. 3(a).

As to the linewidth, we find that the uncoupled linewidth Γ_0 shows a smooth temperature dependence. As shown by the solid curves in Fig. 4(b) this temperature dependence can also be described by a two-phonon-decay model:[32]

$$\Gamma_0(T) = \Gamma(T_0) + C_2[1 + 2n(\omega/2,T)]. \quad (4)$$

In the normal state, the renormalized linewidth ($\Gamma = \Gamma_0 + V^2\rho$) shows a small additional broadening ($V^2\rho \sim 2-3\,cm^{-1}$). The value of Γ_0 is slightly larger for the Zn-doped crystal than that for the Zn-free one. This might be due to the appearance of a new phonon scattering channel as a result of violation of the **k** sum rule by Zn-substitution, while we cannot rule out the possibility of a simple inhomogeneity broadening. Below T_c, the 340-cm^{-1} line exhibits broadening with different temperature dependences for Zn-free and Zn-doped crystals. For a Zn-free crystal, the linewidth Γ reveals a broadening just below T_c, reaches a maximum at $T \sim 75$ K, and turns to narrowing with further cooling below 75 K. For a Zn-doped crystal, the linewidth Γ strongly increases just below T_c and this additional broadening does not disappear with further cooling down to the lowest temperature 10 K.

The difference in Γ(10 K) between Zn-free and Zn-doped YBCO can be explained by the difference in $\rho(\omega)$. That is, as demonstrated in Fig. 2, in the case of a Zn-doped crystal the maximum of the $\rho(\omega)$ function is located closer to 340 cm^{-1} and the peak profile is broader, in comparison with the case of a Zn-free crystal. This leads to a larger broadening $V^2\rho$ ($\omega = 340\,cm^{-1}$) at low temperatures in a Zn-doped crystal than in a Zn-free crystal.

In Fig. 4(c) we plot the temperature dependence of another phonon parameter $S = S_0 + V^2R$. The uncoupled value S_0 shows similar temperature dependences for Zn-free and Zn-doped crystals, except for a small bump at ~ 75 K for the Zn-free case. In contrast, the renormalized parameter S in the superconducting state is quite different for Zn-free and Zn-doped crystals. This difference, due to the term V^2R, is about 2 cm^{-1} at $T = 10$ K which is approximately equal to the difference in the renormalized frequency $\Omega = \Omega_0 + V^2R$ [Fig. 4(a)]

Finally, we examine whether the observed Zn-doping effect can be understood by a conventional pair-breaking theory or not. As demonstrated above, all the changes in the phonon parameters are consistent with the changes in the electronic response shown in Fig. 3, which supports that the spectra are correctly analyzed. The extracted electronic response $\rho(\omega)$ can be compared with the theoretical predictions[1,34] in which strong potential scattering in a unitarity limit is assumed in a *d*-wave superconductor. The low-ω shift of the $\rho(\omega)$ peak, accompanied by the peak broadening, and the increase in the residual $\rho(\omega \to 0)$ qualitatively coincide with the theoretical predictions.[1,34] Estimating the value of $2\Delta_{max}$ from a frequency of the $\rho(\omega)$ peak in the B_{1g} spectrum, the reduction rate of $2\Delta_{max}$ is 460 cm^{-1}/490 $cm^{-1} \approx 0.94$ for the 0.4% Zn doping. Comparing this value with the T_c reduction rate 85 K/93 K ≈ 0.91, we may conclude that 2Δ scales with T_c, just as predicted in a low impurity concentration range by Sun and Maki,[1] although data for many other impurity concentrations are required for a definite conclusion.

Recently, STM measurements revealed that the introduced Zn impurities destroy superconductivity locally around Zn atoms.[16] (Note that this does not mean that superconductivity is not suppressed at all at the sites far from Zn, because the authors in Ref. 16 did not compare the gap values of Zn-free and Zn-doped samples.) From nuclear magnetic resonance measurements, it was reported that the local magnetic moment is induced around Zn.[4] In contrast to these local probes, the Raman measurement probes an average electronic state in a crystal, mainly the electronic state of the matrix far from the impurity sites because the impurity concentration is very low in this study. The present Raman results therefore demonstrate that the superconducting gap is also modified at sites other than the Zn site, which cannot be explained by a simple summation of the spectra for the gap-destroyed area around Zn and the unaffected area far from Zn. The gap suppression at the sites far from Zn was not clear in the STM results on Bi-2212 of Pan *et al.*,[16] but strongly supported by the recent STM measurements on $YBa_2Cu_3O_y$ by Yeh *et al.*[35] As far as the gap value and T_c are concerned, the conventional pair-breaking theory for a *d*-wave superconductor is applicable, on the assumption that Zn acts as a scattering center without any magnetic pair-breaking mechanism.

VI. CONCLUSIONS

We have presented a precise Raman study of the Zn-doping effect on the superconducting gap and phonon renormalization in the twin-free $YBa_2(Cu_{1-x}Zn_x)_3O_{7-\delta}$ single crystals. Using a phenomenological expression for the electronic response function $\chi(\omega) = R(\omega) + i\rho(\omega)$, we successfully separated the coupled and uncoupled phonon parameters and the electronic response function. All the obtained parameters are quite consistent with each other, including T and the impurity dependence.

In the normal state there is no remarkable Zn-doping effect on the Raman spectra except for an increase of the carrier scattering rate observed in the low-ω behavior of $\rho(\omega)$, while below T_c an appreciable change appears even by a small amount ($x = 0.4\%$) of Zn doping. The main change is the low-frequency shift of the $\rho(\omega)$ peak from ~ 490 to ~ 460 cm^{-1}, together with broadening, giving a long tail toward low ω. This electronic change by Zn doping can also be seen in the superconductivity effects on the self-energy of the 340-cm^{-1} line, namely, in the changes of the phonon parameters such as the reduction of softening, the increase of broadening and the decrease of intensity enhancement below T_c.

All these Zn-doping effects can be understood within a framework of the conventional pair-breaking theory for a *d*-wave superconductor in a unitarity limit. Although superconductivity may be most strongly destroyed around the Zn site, the present results indicate that the gap amplitude far

from the Zn site (or the average gap amplitude) is also reduced, roughly scaling with T_c.

ACKNOWLEDGMENTS

The authors are thankful to A. I. Rykov for preparation of the samples. This work was supported by the New Energy and Industrial Technology Development Organization (NEDO) as Collaborative Research and Development of Fundamental Technologies for Superconductivity Applications. One of the authors (D.S.) was supported by a STA fellowship.

APPENDIX: COMPARISON OF THE GREEN'S-FUNCTION FITTING APPROACH AND FANO FITTING APPROACH

By simply rearranging Eq. (1), one can easily obtain the following expression for the Raman intensity based on the Green's-function operator approach:

$$I(\omega)=[1+n(\omega)]\left\{\rho(\omega)\frac{\Gamma_0}{\Gamma}+\frac{V^2\rho(\omega)^2}{\Gamma(1+\varepsilon^2)}\left[\left(\frac{S}{V^2\rho(\omega)}+\varepsilon\right)^2\right]\right\}. \quad \text{(A1)}$$

If only renormalized phonon parameters are of interest, then a simpler formula for the coupled Raman spectrum can be used:[20]

$$I(\omega)=[1+n(\omega)]\left\{(\text{Fano background})+\frac{I_0}{(1+\varepsilon^2)}[(q+\varepsilon)^2]\right\}. \quad \text{(A2)}$$

This formula describes the case of the interaction of a sharp state with a broad continuum first considered by Fano.[36] Here $\varepsilon=(\omega-\Omega)/\Gamma$ is the same as in Eq. (A1) and $q=(VT_p/T_e+V^2R)/\Gamma$ is called the Fano parameter. We fitted the spectral region around the 340-cm^{-1} phonon line using the Fano approach [Eq. (A2)], with a "Fano background" $=C_0+C_1\omega+C_2\omega^2$. To calculate the temperature dependence of the total phonon intensity based on the Fano approach, one uses the following formula:[37,38]

$$I_p=\pi I_0\Gamma q^2=\pi I_0(VT_p/T_e+V^2R)^2/\Gamma\sim S^2. \quad \text{(A3)}$$

Equation (A3) shows that the phonon intensity is determined by an interband electronic excitation via the matrix elements T_p (bare phonon intensity), as well as by a coupling to the Raman-active electronic continuum via the term V^2R.

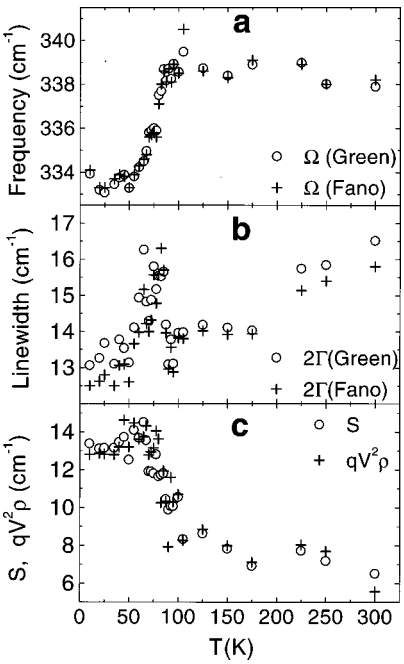

FIG. 5. Comparison of the 340-cm^{-1} phonon line parameters obtained from the Fano fitting procedure and from the Green function fitting procedure for the Zn-free crystal. (a) The renormalized frequencies $\Omega=\Omega_0+V^2R$. (b) The renormalized linewidth $2\Gamma=2(\Gamma_0+V^2\rho)$. (c) The renormalized parameter $S=S_0+V^2R$, and the $qV^2\rho$ parameter.

By comparing Eqs. (A1) and (A2), one can see that the formulas based on the Green's-function approach and on the Fano approach become equivalent if

$$(\text{Fano background})=\rho\frac{\Gamma_0}{\Gamma},\quad I_0=\rho\frac{\Gamma-\Gamma_0}{\Gamma},$$

$$S=qV^2\rho=q(\Gamma-\Gamma_0). \quad \text{(A4)}$$

In Fig. 5 we show a set of the Fano fitting parameters together with the Green's-function fitting parameters. We can see a strong correlation of the results obtained by the two approaches. The temperature dependencies of the renormalized frequency Ω and 2Γ, as well as of S and $qV^2\rho$ parameters, are essentially the same for the Fano and Green approaches, as expected from Eq. (A4). Therefore, both approaches give the same renormalized phonon parameters (frequency, linewidth, and intensity), if we assume an appropriate background function. A disadvantage of the Fano fitting approach is that the electronic parameters cannot be determined.

*Permanent address: A. F. Ioffe Physical-Technical Institute, 194021 St. Petersburg, Russia.

[1] Y. Sun and K. Maki, Phys. Rev. B **51**, 6059 (1995).

[2] R. J. Radtke, K. Levin, H.-B. Schutter, and M. R. Norman, Phys. Rev. B **48**, 653 (1993).

[3] H. Alloul, P. Mendels, H. Casalta, J. F. Marucco, and J. Arabski, Phys. Rev. Lett. **67**, 3140 (1991).

[4] M.-H. Julien, T. Fehér, M. Horvatic, C. Berthier, O. N. Bakharev, P. Ségransan, G. Collin, and J.-F. Marucco, Phys. Rev. Lett. **84**, 3422 (2000).

[5] Y. Fukuzumi, K. Mizuhashi, K. Takenaka, and S. Uchida, Phys. Rev. Lett. **76**, 684 (1996).

[6] C. Panagopoulos, J. R. Cooper, N. Athanassopoulou, and J. Chrosch, Phys. Rev. B **54**, R12721 (1996).
[7] J. W. Loram, K. A. Mirza, J. M. Wade, J. R. Cooper, and W. Y. Liang, Physica C **235–240**, 134 (1994).
[8] D. N. Basov, B. Dabrowski, and T. Timusk, Phys. Rev. Lett. **81**, 2132 (1998).
[9] N. L. Wang, S. Tajima, A. I. Rykov, and K. Tomimoto, Phys. Rev. B **57**, R11 081 (1998).
[10] K. Kakurai, S. Shamoto, T. Kiyokura, M. Sato, J. M. Tranquada, and G. Shirane, Phys. Rev. B **48**, 3485 (1993).
[11] C. Bernhard, J. L. Tallon, C. Bucci, R. De Renzi, G. Guidi, G. V. M. Williams, and Ch. Niedermayer, Phys. Rev. Lett. **77**, 2304 (1996).
[12] E. Altendorf, J. C. Irwin, W. N. Hardy, and R. Liang, Physica C **185–189**, 1375 (1991).
[13] A. Matic, M. Käll, L. Börjesson, and Y. Eltsev, J. Phys. Chem. Solids **56**, 1835 (1995).
[14] M. F. Limonov, S. Tajima, and A. Yamanaka, in *Advances in Superconductivity XII*, edited by T. Yamashita and K. Tanabe, (Springer-Verlag, Tokyo, 2000), p. 269.
[15] M. Limonov, D. Shantsev, S. Tajima, and A. Yamanaka, Physica C **357-360**, 265 (2001).
[16] S. H. Pan, E. W. Hudson, K. M. Lang, H. Eisaki, S. Uchida, and J. C. Davis, Nature (London) **403**, 746 (2000).
[17] For a review, see M. Cardona, Physica C **317–318**, 30 (1999); D. Branch and J. P. Carbotte, J. Supercond. **13**, 535 (2000).
[18] R. Zeyher and G. Zwicknagl, Solid State Commun. **66**, 617 (1988); R. Zeyher and G. Zwicknagl, Z. Phys. B: Condens. Matter **78**, 175 (1990).
[19] E. J. Nicol, C. Jiang, and J. P. Carbotte, Phys. Rev. B **47**, 8131 (1993).
[20] C. Thomsen, in *Light Scattering in Solids* VI, edited by M. Cardona and G. Guntherodt (Springer-Verlag, Berlin, 1991).
[21] M. F. Limonov, A. I. Rykov, S. Tajima, and A. Yamanaka, Phys. Rev. B **61**, 12 412 (2000).
[22] A. I. Rykov, W. J. Jang, H. Unoki, and S. Tajima, in *Advances in Superconductivity VIII*, edited by H. Hayakawa and Y. Enomoto (Springer-Verlag, Tokyo, 1996), p. 341.
[23] D. R. Wake, F. Slakey, M. V. Klein, J. P. Rice, and D. M. Ginsberg, Phys. Rev. Lett. **67**, 3728 (1991).
[24] A. G. Panfilov, M. F. Limonov, A. I. Rykov, S. Tajima, and A. Yamanaka, Phys. Rev. B **57**, R5634 (1998).
[25] X. K. Chen, E. Altendorf, J. C. Irwin, R. Liang, and W. N. Hardy, Phys. Rev. B **48**, 10 530 (1993).
[26] X. K. Chen, J. C. Irwin, R. Liang, and W. N. Hardy, Physica C **227**, 113 (1994).
[27] T. P. Devereaux, A. Virosztek, and A. Zawadowski, Phys. Rev. B **51**, 505 (1995).
[28] T. Strohm and M. Cardona, Phys. Rev. B **55**, 12 725 (1997).
[29] A. Bock, S. Ostertun, R. Das Sharma, M. Rübhausen, K.-O. Subke, and C. T. Rieck, Phys. Rev. B **60**, 3532 (1999).
[30] A. Bock, Ann. Phys. (Leipzig) **8**, 441 (1999).
[31] T. P. Devereaux, D. Einzel, B. Stadlober, R. Hackl, D. H. Leach, and J. J. Neumeier, Phys. Rev. Lett. **72**, 396 (1994).
[32] M. Balkanski, R. F. Wallis, and E. Haro, Phys. Rev. B **28**, 1928 (1983).
[33] E. Altendorf, X. K. Chen, J. C. Irwin, R. Liang, and W. N. Hardy, Phys. Rev. B **47**, 8140 (1993).
[34] T. P. Devereaux and A. P. Kampf, Phys. Rev. B **61**, 1490 (2000).
[35] N.-C. Yeh, C.-T. Chen, G. Hammerl, J. Mannhart, S. Tajima, K. Yoshida, A. Schmehl, C. W. Schneider, and R. R. Schulz, Phys. Rev. Lett. **87**, 087003 (2001).
[36] U. Fano, Phys. Rev. **124**, 1866 (1961).
[37] M. Chandrasekhar, H. R. Chandrasekhar, M. Grimsditch, and M. Cardona, Phys. Rev. B **22**, 4825 (1980).
[38] V. G. Hadjiev, X. Zhou, T. Strohm, M. Cardona, Q. M. Lin, and C. W. Chu, Phys. Rev. B **58**, 1043 (1998).